

# Theoretical Debye–Waller factors of $\alpha$ -MoO<sub>3</sub> estimated by an equation-of-motion method

W.-J. Chun,<sup>a,b</sup> K. Ijima,<sup>c</sup> Y. Ohminami,<sup>a</sup> S. Suzuki<sup>a,b</sup> and K. Asakura<sup>a\*</sup>

<sup>a</sup>Catalysis Research Center, Hokkaido University, Kita-ku, Sapporo 060-0811, Japan, <sup>b</sup>Core Research for Evolutional Science and Technology, Japan Science and Technology Corporation, Japan, and <sup>c</sup>Department of Electrical Engineering, Yamanashi University, Kofu 400-8511, Japan.  
E-mail: askr@cat.hokudai.ac.jp

EXAFS oscillations of MoO<sub>3</sub>, which has a highly asymmetric local structure, have been calculated using backscattering amplitudes and phase shifts derived from the *FEFF8* code and using Debye–Waller factors from an equation-of-motion method. They were compared with polarization-dependent empirical EXAFS data of the  $\alpha$ -MoO<sub>3</sub> single crystal at various temperatures. The theoretical EXAFS oscillations of Mo–O bonds for the [001] direction of the single crystal, where two symmetric Mo–O bonds exist, reproduced well the experimental data. On the other hand, the calculated data for the [100] direction, which contain two asymmetric Mo–O bonds with different bond lengths, agree well with the experimental data only after adjustment of the amplitude reduction factors for different Mo–O bonds. EXAFS oscillations of MoO<sub>3</sub> powder were also calculated by the same method, and theoretical parameters that could reproduce the experimental data were found. These results suggest that the equation-of-motion method can evaluate the Debye–Waller factors efficiently in molecules with asymmetric local structures and can reduce curve-fitting parameters.

**Keywords:** EXAFS; polarization-dependent EXAFS; temperature-dependent EXAFS; Debye–Waller factors; equation of motion; MoO<sub>3</sub> single crystals.

## 1. Introduction

Extended X-ray absorption fine structure (EXAFS) has been widely used as a powerful tool for analyzing the structures of the chemical compounds in matrices like solutions and solids. Its feasibility, however, is limited to highly symmetrical systems containing only one or two bond lengths in one shell. In a system containing an atom surrounded by atoms with various bond distances, as is often found in metal oxides, it is rather difficult to obtain the complete structure information only from EXAFS.

For example, MoO<sub>3</sub> is one of the important catalyst materials and many EXAFS studies have been carried out. The Mo atom is surrounded by O atoms with several different Mo–O bond lengths. Actually, even in an authentic compound, MoO<sub>3</sub> has five different Mo–O bond lengths in the first shell, as shown in Fig. 1. In principle, the bond length and coordination number for each shell could be determined by multishell non-linear least-square fitting analysis of EXAFS. The curve-fitting analysis of EXAFS oscillations,  $\chi(k)$ , is usually carried out using equations (1) and (2) (Teo, 1986),

$$\chi(k) = \sum_i \frac{S_{0i}^2 N_i F_i(k_i)}{k_i r_i^2} \exp(-2\sigma_i^2 k_i^2) \exp(-2r_i/\lambda_i) \times \sin[2k_i r_i + \varphi_i(k_i)], \quad (1)$$

$$k_i = [k^2 + (2m\Delta E_{0i}/\hbar^2)]^{1/2}, \quad (2)$$

where  $S_{0i}$ ,  $N_i$ ,  $r_i$ ,  $\sigma_i$  and  $\lambda_i$  are the amplitude reduction factor, coordination number, interatomic distance, Debye–Waller factor and inelastic mean free path for the  $i$ th shell, respectively. The parameters  $F_i(k)$  and  $\varphi_i(k)$  are the amplitude and phase-shift functions, respectively.  $\lambda_i$ ,  $F_i(k)$  and  $\varphi_i(k)$  can be obtained from *ab initio* EXAFS calculations such as the *FEFF* code. The amplitude reduction factor  $S_{0i}$  is obtained by using the experimental values of reference samples.  $\Delta E_{0i}$  is an energy shift in the origin of the photoelectron kinetic energy for the  $i$ th shell and optimized using equation (2). The four parameters  $N_i$ ,  $\sigma_i$ ,  $r_i$  and  $\Delta E_{0i}$  per shell are used as curve-fitting parameters in EXAFS analysis. Thus, in the complicated system where multishell fitting is necessary, a lot of fitting parameters make it extremely difficult to derive a reliable structure from EXAFS owing to the limitation of the number of independent fitting parameters,  $N_{\text{ind}} = (2\Delta k \Delta r/\pi) + 2$ , where  $\Delta k$  and  $\Delta r$  are the width of the Fourier transformation in the  $k$  and  $r$  space, respectively, as well as creating a correlation problem between fitting parameters. This major drawback of the curve-fitting method can be improved if certain fitting parameters are fixed. To alleviate, albeit partially, these problems,  $\Delta E_{0i}$  can be fixed to that of a reference compound. We reported the reasonable curve-fitting results for the first nearest Mo–O bonds of  $\alpha$ -MoO<sub>3</sub> powder with three fixed  $\Delta E_0$  parameters that were estimated from reference compounds (Ijima *et al.*, 2002). Another parameter we propose here to fix is the Debye–Waller (DW) factor. The DW factor accounts for thermal and structural disorder and generally dampens EXAFS oscillations with respect to increasing photoelectron energy, and thus it can significantly complicate the analysis to derive accurate coordination numbers. Recently, Poiarkova *et al.* proposed the equation-of-motion (EM) method as an efficient approach to evaluate the thermal DW factor in terms of a few local force constants in an aperiodic system (Poiarkova & Rehr, 1997, 1999a,b; Krappe & Rossner, 2002). They presented advantages of the EM method in a highly symmetric system such as Cu, Ge and zinc tetraimidazole, but there was no discussion for more complicated or asymmetric structures such as MoO<sub>3</sub>.

In this work we have applied the EM method to the analysis of MoO<sub>3</sub> in order to check the validity of the EM method for an asymmetric system. To simplify the evaluation, we first analyzed polarization-dependent EXAFS spectra of a single-crystal MoO<sub>3</sub> and then examined powder MoO<sub>3</sub>. With a little modification in amplitude, we have found that the EM method is very powerful for analyzing a compound with asymmetrical molecular structure.

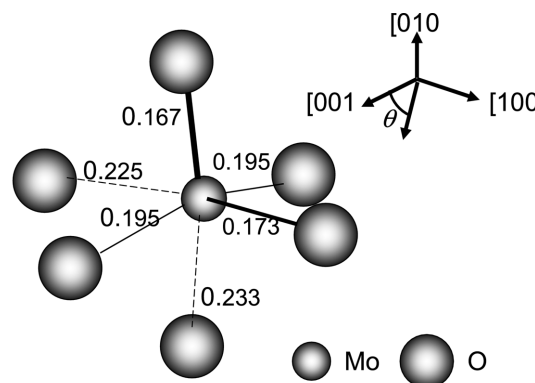


**Figure 1**  
Local structure of octahedron MoO<sub>3</sub> in crystalline  $\alpha$ -MoO<sub>3</sub> (Kihlberg, 1963). Dimensions of bond lengths: nm.

2. Experimental

An  $\alpha$ -MoO<sub>3</sub> (010) single crystal was prepared by a MoO<sub>3</sub>-Na<sub>2</sub>CO<sub>3</sub> flux method (Balakumar & Zeng, 1998), and was verified by a powder X-ray diffraction technique (Ijima *et al.*, 2002). The prepared single crystal had a thin-plate geometry normal to the [010] direction with dimensions of 1 mm × 8 mm. EXAFS was measured in transmission mode at the BL10B at the Photon Factory of the Institute of Material Structure Science (Proposal No. 98-G303). The ring energy and current were 2.5 GeV and 300 mA, respectively. The X-ray was monochromated with a Si (311) channel-cut monochromator and detected by two ionization chambers filled with Ar/N<sub>2</sub> (50:50) for  $I_0$  and Ar 100% for  $I$ . The prepared sample was mounted on a goniometer for obtaining polarization-dependent EXAFS and adjusted with the [010] direction parallel to the incident X-ray. The crystal orientation  $\theta$  was defined as 0° when the electric vector of the incident X-ray was in the [001] direction of the crystal as shown in Fig. 1. The inaccuracy of the crystal orientation was estimated to within 5°. Data analysis was carried out using REX2000, an EXAFS analysis program package coded by Rigaku, Japan. The backscattering amplitude and the phase shift were theoretically calculated by the FEFF8.1 code (Ankudinov *et al.*, 1998; Ankudinov & Rehr, 2000). Polarization dependence was also considered during the calculations. The DW factor was estimated by an EM code implemented in FEFF8.1 (Poiarkova & Rehr, 1997, 1999a,b). The force constants of  $\alpha$ -MoO<sub>3</sub> used in the calculations were obtained from the experimental Raman spectroscopy results (Py & Maschke, 1981).

3. Results and discussions

Figs. 2 and 3 show, respectively, the oscillations and their Fourier transforms of the temperature- and polarization-dependent EXAFS oscillations of  $\alpha$ -MoO<sub>3</sub> for the [001] and the [100] directions. The Fourier transforms consist of roughly two peaks, *i.e.* Mo–O and Mo–Mo in the ranges 0.1–0.2 nm and 0.3–0.4 nm, respectively. There is stronger temperature dependence in the Mo–Mo peak than in the Mo–O peak. This means that the thermal vibration in the Mo–Mo bond is larger than that in Mo–O. A single peak appears in the Mo–O region of [001] which corresponds to the Mo–O bond at 0.195 nm, while a doublet peak is found for [100] corresponding to the two Mo–O bonds at 0.173 and 0.225 nm as shown in Fig. 1.

Fig. 4(a) shows the Fourier-filtered experimental (solid) and theoretical (dotted) EXAFS oscillations for the [001] direction in the first nearest neighbour. The theoretical oscillations were obtained based on FEFF8 together with the EM method. There are two equivalent Mo–O bonds in the [001] direction. The calculated curve agrees well with the experiments at all temperatures. We can safely say that the EM method can estimate the DW factor and its temperature dependence correctly in the symmetrical bonds as reported previously (Poiarkova & Rehr, 1997, 1999a,b). Fig. 4(b) shows the experimental (solid) and theoretical (dotted) EXAFS oscillations for the [100] direction. This direction contains two different Mo–O bonds of 0.173 and 0.225 nm. The theoretical EXAFS oscillations were in poor agreement with the experiments compared with the results in the [001] direction. FEFF8 especially failed to reproduce characteristic shoulders appearing at around  $k = 80 \text{ nm}^{-1}$ . We optimized the theoretical EXAFS by adjusting the Mo–O bond lengths but little improvement was found. Thus, the FEFF8 and the EM method cannot directly simulate the EXAFS data for the asymmetric bonds. The shoulder structure at  $k = 80 \text{ nm}^{-1}$  was enhanced at 30 K. Fig. 3(b) shows that the longer distance Mo–O peak appearing at 0.19 nm increases with a decrease of the

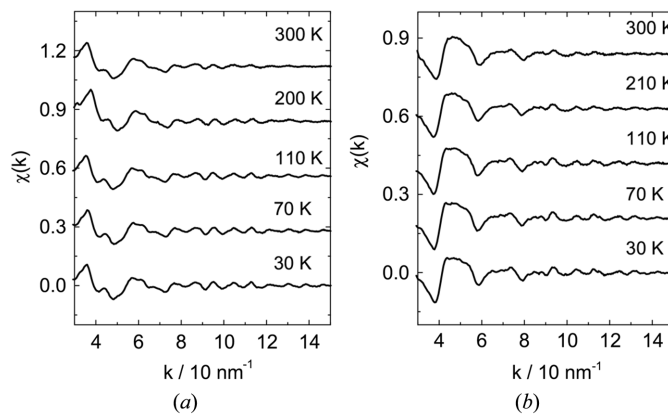


Figure 2 EXAFS oscillations at various temperatures for (a) the [001] direction and (b) the [100] direction. Dimensions are in nm.

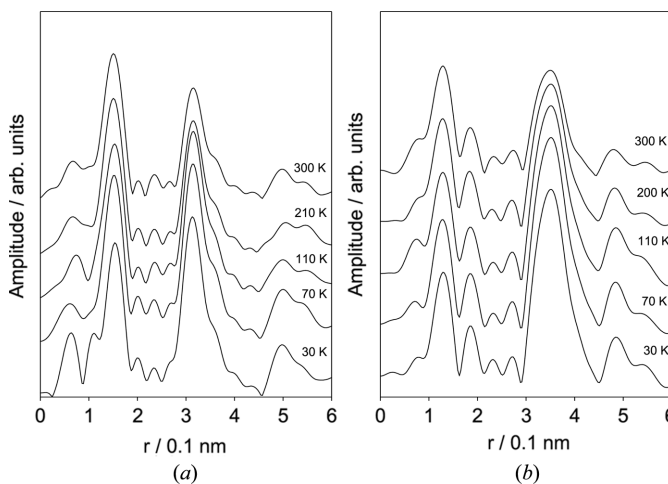


Figure 3 Fourier transforms of the  $k^3$ -weighted EXAFS oscillations at various temperatures for (a) the [001] direction and (b) the [100] direction. The Fourier range is  $30\text{--}130 \text{ nm}^{-1}$ .

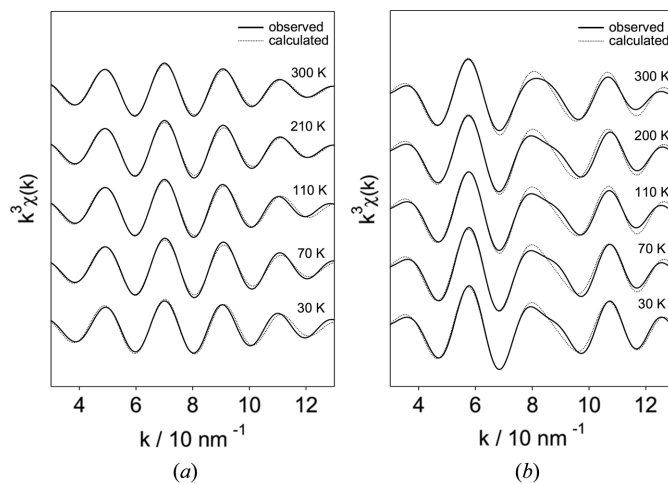
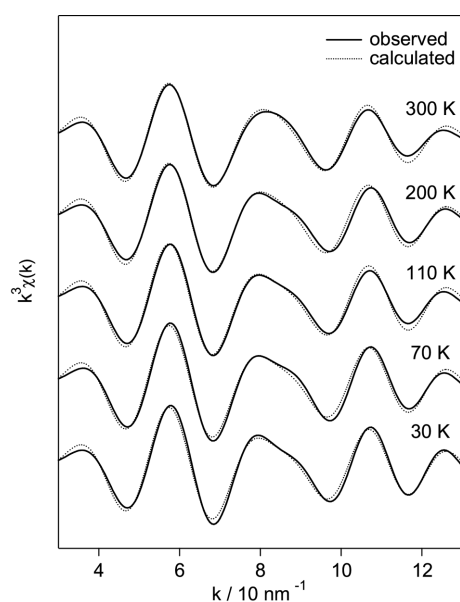


Figure 4 Observed  $k^3$ -weighted Fourier-filtered oscillations (solid line) and calculated (dotted line) for (a) the [001] direction and (b) the [100] direction. The Fourier-filtering range is  $r = 0.11\text{--}0.18 \text{ nm}$  for the [001] direction and  $r = 0.08\text{--}0.22 \text{ nm}$  for the [100] direction. The measurement temperatures are shown.

temperature. Thus the shoulder structure should arise from the longer Mo—O bond. In fact, the EM calculation indicated that the DW factor for the longer Mo—O bond decreased much more than that for the shorter bond as the temperature decreased. The origin of the shoulder structure was mainly from the longer Mo—O bond. The reason why the *FEFF8* code in the [100] direction could not reproduce the data might be due to the small contribution of the longer Mo—O bond to the EXAFS oscillation. The EXAFS amplitude is a product of the backscattering amplitude  $F_i(k)$  and inelastic loss factors [ $S_{0i}$  and  $\exp(-2r_i/\lambda_i)$ ].  $F_i(k)$  and  $\exp(-2r_i/\lambda_i)$  are calculated using the *FEFF* code.  $F_i(k)$  depends strongly on the atomic number  $Z$  and weakly on the chemical state and the bond distance. This dependency has been demonstrated empirically by the transferability of  $F_i(k)$  between the same atomic pair. Since we can reproduce the EXAFS oscillations in the [001] direction successfully using *FEFF8* in the [100] direction, poor estimation of  $F_i(k)$  is not the reason for the failure to reproduce the oscillation. The intrinsic loss factor  $S_{0i}$ , which arises from the passive electron effect, can be rationally regarded as the same for the same central atom (Teo, 1986). On the other hand, the inelastic mean free path  $\lambda_i$  should depend on the electron density in the photoelectron path. In the *FEFF8* calculation,  $\lambda_i$  is treated as a constant in the whole direction owing to the muffin-tin approximation (Rehr *et al.*, 1991). This means that the same  $\lambda_i$  is applied to two Mo—O bonds which have different electron densities. In the first approximation,  $\text{Mo}^{6+}$  is surrounded by six  $\text{O}^{2-}$  ions with different bond lengths. Thus, the electron density between Mo and O is higher in the shorter Mo—O bond and hence  $\lambda_i$  should be smaller and the damping term  $\exp(-2r_i/\lambda_i)$  should be larger in the shorter bond. To verify this hypothesis, we calculated  $\lambda_i$  for Mo—O bonds independently using *FEFF* assuming two virtual symmetric  $\text{MoO}_6$  octahedra with their Mo—O bonds equal to 0.173 nm and 0.225 nm. Then we calculated the amplitude ratio of the exponential damping term  $\exp(-2r_i/\lambda_i)$  for the Mo—O bond of 0.225 nm to that for the Mo—O bond of 0.176 nm. Consequently, the ratio was about 1.1, indicating that the exponential damping term for a Mo—O bond length of 0.225 nm was smaller and consistent with our prediction. We multi-



**Figure 5** Observed  $k^3$ -weighted Fourier-filtered oscillations (solid line) and the optimized calculated ones (dotted line) for the [100] direction. The Fourier-filtering range is  $r = 0.08$ – $0.22$  nm. The measurement temperatures are shown.

**Table 1** Curve-fitting parameters for  $\alpha$ - $\text{MoO}_3$  powder.

Shell	$N^\dagger$	$r$ (nm)		$\sigma^2$ ( $\times 10^{-5}$ nm $^2$ ) $^\dagger$	$\Delta E_0$ (eV) $^\dagger$	$R_{\text{factor}}$ (%)
		EXAFS	X-ray $^\ddagger$			
Mo—O	1	$0.165 \pm 0.002$	0.167	1.34	0	1.17
Mo—O	1	$0.175 \pm 0.002$	0.173	1.74	0	
Mo—O	2	$0.195 \pm 0.002$	0.195	3.51	0	
Mo—O	1	$0.226 \pm 0.002$	0.225	6.38	0	
Mo—O	1	$0.235 \pm 0.002$	0.233	6.39	0	

$^\dagger$  Fixed curve-fitting parameters.  $^\ddagger$  From Kihlberg (1963).

plied the calculated EXAFS oscillations arising from the Mo—O bond length of 0.225 nm by a factor of 1.1. After the longer Mo—O distance was optimized within the acceptable error bar to be 0.227 nm, we could reproduce the shoulder structure and found excellent agreement between the experimental and theoretical oscillations, as shown in Fig. 5. These results have demonstrated that a small amplitude modification is necessary in order to calculate the EXAFS oscillations of asymmetric systems, and the modification value can be estimated from the inelastic mean free path.

We then calculated the EXAFS oscillation of  $\alpha$ - $\text{MoO}_3$  powder measured at 300 K. The amplitude and phase-shift functions were calculated from *FEFF8* and the DW factors were derived from the EM method. The Fourier-filtered EXAFS oscillations (solid) agreed well with the calculated ones (dotted), as shown in Fig. 6. Five bond lengths for Mo—O are used as fitting parameters and the residual in the fitting,  $R = \sum [\chi_{\text{obs}}(k) - \chi_{\text{cal}}(k)]^2 / \sum \chi_{\text{obs}}(k)^2$ , was 0.017. The bond lengths are in good agreement with the crystallographic data within the error bars, as shown in Table 1. In our previous work we carried out a curve-fitting analysis of the same data using phase-shift and amplitude functions empirically derived from the polarization-dependent EXAFS spectra of  $\text{MoO}_3$  (Ijima *et al.*, 2002). In this case we used nine fitting parameters, *i.e.* three Mo—O shells, each of which contained three fitting parameters ( $N, r, \sigma$ ), and obtained  $R = 0.052$  in the same fitting condition. Thus, the *FEFF8*-derived parameters and EM-calculated DW factors can reproduce the experimental EXAFS much better than the empirically derived parameters. These results demonstrated that the EM method can evaluate the DW factor successfully even in a complicated asymmetric system only by adjusting the inelastic loss factor. This is a great advantage for those who are struggling to derive exact structures of complicated chemical

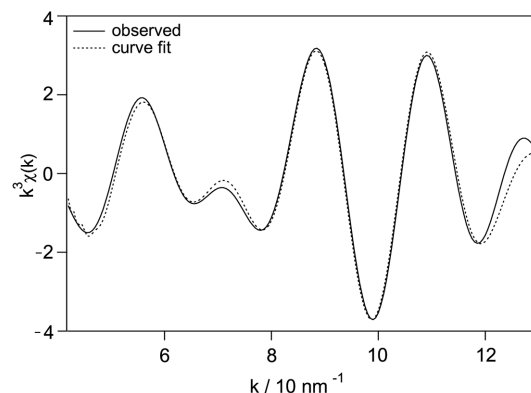


**Figure 6** Observed  $k^3$ -weighted Fourier-filtered oscillation (solid line) and the best fit (dotted line) for  $\text{MoO}_3$  powder. The Fourier-filtering range is  $r = 0.08$ – $0.22$  nm.

substances from EXAFS oscillations. We can estimate the force constants of many inorganic compounds experimentally from vibrational data (Nakamoto, 1986). In addition, the force constant has a strong correlation with the bond distances (Yokoyama *et al.*, 1994; Hardcastle & Wachs, 1990, 1991). In some oxides, the relation between force constants and bond distances are graphically given (Hardcastle & Wachs, 1990, 1991). Recent developments in *ab initio* calculations, such as *Gaussian98* (see <http://www.gaussian.com>), may allow us to evaluate the force constants based on the chemical state and the bond distance correctly. Using this relation and the EM method, we can reduce the fitting parameters by correlating the DW factor directly with the corresponding bond distance. Consequently, we can increase the reliability of the multishell curve-fitting analysis.

This work was financially supported by a NEDO international grant (2001-EF011).

## References

- Ankudinov, A. L., Ravel, B., Rehr, J. J. & Conradson, S. D. (1998). *Phys. Rev. B*, **58**, 7565–7576.
- Ankudinov, A. L. & Rehr, J. J. (2000). *Phys. Rev. B*, **62**, 2437–2445.
- Balakumar, S. & Zeng, H. C. (1998). *J. Cryst. Growth*, **194**, 195–202.
- Hardcastle, F. D. & Wachs, I. E. (1990). *J. Raman Spectrosc.* **21**, 683.
- Hardcastle, F. D. & Wachs, I. E. (1991). *J. Phys. Chem.* **95**, 5031.
- Ijima, K., Ohminami, Y., Suzuki, S. & Asakura, K. (2002). *Top. Catal.* **18**, 125–127.
- Kihlberg, L. (1963). *Ark. Kemi.* **21**, 357.
- Krappe, H. J. & Rossner, H. H. (2002). *Phys. Rev. B*, **66**, 184303-1–184303-20.
- Nakamoto, K. (1986). *Infrared and Raman Spectra of Inorganic and Coordination Compounds*, 4th ed. New York: John Wiley.
- Poiarkova, A. V. & Rehr, J. J. (1997). *J. Phys. IV*, **7**(C2), 155–156.
- Poiarkova, A. V. & Rehr, J. J. (1999a). *Phys. Rev. B*, **59**, 948–957.
- Poiarkova, A. V. & Rehr, J. J. (1999b). *J. Synchrotron Rad.* **6**, 313–314.
- Py, M. A. & Maschke, K. (1981). *Physica B*, **105**, 370–374.
- Rehr, J. J., Mustre de Leon, J., Zabinsky, S. I. & Albers, R. C. (1991). *J. Am. Chem. Soc.* **113**, 5135–5140.
- Teo, B. K. (1986). *EXAFS: Basic Principles and Data Analysis*. New York: Springer-Verlag.
- Yokoyama, T., Hamamatsu, H., Kitajima, Y., Takata, Y., Yagi, S. & Ohta, T. (1994). *Surf. Sci.* **313**, 197–208.